Environmental Modelling & Software 62 (2014) 454–464

Contents lists available at ScienceDirect

Environmental Modelling & Software

journal homepage: www.elsevier.com/locate/envsoft

Dynamic assessment of the impact of drought on agricultural yield and scale-dependent return periods over large geographic regions☆

Chaoqing Yu [a, *], Changsheng Li [a, b], Qinchuan Xin [a], Han Chen [a], Jie Zhang [a], Feng Zhang [c], Xuecao Li [a], Nick Clinton [a], Xiao Huang [a], Yali Yue [a], Peng Gong [a, d]

[a] Center for Earth System Science, Key Lab of Earth System Numerical Simulation, Tsinghua University, Beijing, China
[b] Institute for the Study of Earth, Oceans, and Space, University of New Hampshire, USA
[c] State Key Laboratory of Pastoral Agricultural Ecosystem, Lanzhou University, Lanzhou, Gansu, 730000, China
[d] Joint Center for Global Change Studies, Beijing, 100875, China

ARTICLE INFO

Article history:
Received 30 September 2013
Received in revised form
8 July 2014
Accepted 7 August 2014
Available online 4 September 2014

Keywords:
Drought
Yield prediction
Dynamic
Return period
Scale

ABSTRACT

Agricultural droughts can create serious threats to food security. Tools for dynamic prediction of drought impacts on yields over large geographical regions can provide valuable information for drought management. Based on the DeNitrification-DeComposition (DNDC) model, the current research proposes a Drought Risk Analysis System (DRAS) that allows for the scenario-based analysis of drought-induced yield losses. We assess impacts on corn yields using two case studies, the 2012 U.S.A. drought and the 2000 and 2009 droughts in Liaoning Province, China. The results show that the system is able to perform daily simulations of corn growth and to dynamically evaluate the large-scale grain production in both regions. It is also capable of mapping the up-to-date yield losses on a daily basis, the additional losses under different drought development scenarios, and the yield-based drought return periods at multiple scales of geographic regions. In addition, detailed information about the water-stress process, biomass development, and the uncertainty of drought impacts on crop growth at a specific site can be displayed in the system. Remote sensing data were used to map the areas of drought-affected crops for comparison with the modeling results. Beyond the conventional drought information from meteorological and hydrological data, this system can provide comprehensive and predictive yield information for various end-users, including farmers, decision makers, insurance agencies, and food consumers.

1. Introduction

Drought is a recurring natural hazard (Wilhite and Buchanan-Smith, 2005) that can cause widespread damage to agricultural production. Although studies in quantitative drought evaluations have been conducted for almost a century (e.g., Munger, 1916; Kincer, 1919; Marcovitch, 1930), the capacity for decision support in actual drought management is still limited. For example, during an agricultural drought before harvest, questions frequently asked by decision makers include: how much yield reduction the drought has caused to date; how severe it is in relation to previous droughts (return periods); and what the consequences would be if the drought continues? There is no current body of literature that seeks to fully address these questions in a quantitative way, especially in large-scale agricultural droughts.

The underlying challenge behind these questions is how to address the uncertainty of drought development and quantify its impacts on grain yields. The stochastic nature of drought is an inherent cause of uncertainty (Refsgaard et al., 2007). It is difficult to achieve a deterministic prediction of changes in drought severity because droughts develop slowly and last a long time. Another important source of uncertainty is from the epistemic constraints. Drought is often a phenomenon without a clearly defined beginning or end (Whilhite, 2005). The complex mechanisms of how the drought affects the processes of water, soil, and crop growth are not well understood. Although there are multiple approaches that are relevant to agricultural drought management for the quantitative evaluation of drought severity and effects, the dynamic evaluation of the uncertainties in predicting the drought impacts on yield losses has not been well studied.

☆ Thematic Issue on Agricultural Systems Modeling & Software.

* Corresponding author.
E-mail addresses: chaoqingyu@tsinghua.edu.cn, chaoqingyu@gmail.com (C. Yu).

http://dx.doi.org/10.1016/j.envsoft.2014.08.004

The primary methods available for quantifying drought severity and yield impacts include agricultural surveys, drought severity indices, remote sensing and crop modeling. Agricultural surveys are still the basic means for obtaining information on crop-growth status and for predicting grain yield in most countries. For instance, in the U.S.A., the National Agricultural Statistics Service (NASS) of the U.S. Department of Agriculture (USDA) makes monthly predictions of agricultural yields based on statistical analyses of routine survey data. The survey includes in-field observations of crop conditions in major crop-producing states, as well as interviews with 5500–27,000 farm operators via mail or phone calls (NASS, 2009a). Due to independent and unbiased data collection for decades, the monthly yield projection based on regression analysis produce accurate results when compared to final yield reports. However, in places lacking reliable and consistent long-term historical data, this approach is not feasible.

Various drought indicators have been developed to automatically classify drought severity since the 20th century (Heim Jr. 2002). The indices relevant to agricultural drought are usually based on the parameters of precipitation, soil moisture, and transpiration. These indices include MAI (moisture adequacy index, McGuire and Palmer, 1957), CMI (crop moisture index, Palmer, 1968), CWSI (crop water stress index, Idso et al., 1981), SPI (standard precipitation index, McKee et al., 1993), SMDI (soil moisture deficit index, Narasimhan and Srinivasan, 2005), SMI (soil moisture index, Hunt et al., 2009), and ARID (the Agricultural Reference Index for Drought, Woli et al., 2012). Comprehensive drought indices such as PDSI (Palmer Drought Severity Index, Palmer, 1965) and DM (Drought Monitor, Svoboda, 2000) also provide important information for agricultural drought management. There are multiple drought indices that are based on information from remote sensing data, such as VCI (vegetation condition index, Kogan, 1995), and NDWI (the normalized difference water index, Gao, 1996) for classifying drought severity. Remote sensing has also been applied to crop yield predictions (NASS, 2009b). The methods usually relate historical records of crop yields to vegetation indices derived from remote sensing data (Murthy et al., 1996; Kogan et al., 2005; Sakamoto et al., 2013). However, this approach is constrained to the time frame and geographical area of the study. Though some regression-based models have been successfully generalized to new areas, the nature of these methods is empirical, and they are unlikely to predict crop yields under extreme conditions that are beyond historical records (Moulin et al., 1998; Becker-Reshef et al., 2010; Bolton and Friedl, 2013).

Crop models are considered to be valuable tools for improving agricultural management and decision making. Most crop models predict yields based on simulating physiological processes during crop growth. These models include ELCROS (de Wit, 1965), CERES (Jones and Kiniry, 1986), EPIC (Williams and Singh, 1995), APSIM (McCown et al., 1996), ALMANAC (Kiniry et al., 1996), WOFOST (Boogaard et al., 1998; Eitzinger et al., 2004), and AquaCrop (Steduto et al., 2009). Another branch of models have been developed for simulating the biogeochemical processes such as carbon, hydrogen, oxygen, nitrogen, and phosphorus cycles in agro-ecosystems. Simulating crop growth to predict yields is also an essential part of these biogeochemical models, such as DNDC (Li et al., 2006; Zhang et al., 2002) and Century (Gilmanov et al., 1997). Many of these models have been developed and evaluated at the field scale rather than for large geographic regions (Palosuo et al., 2011). Most existing crop models are complex, and require a large number of input parameters that are not readily available (Steduto et al., 2009). Without establishing detailed agricultural databases, it is difficult to apply these models for large-scale simulations of crop growth.

One strength of using crop models for yield prediction is that the models allow for a sensitivity analysis (Saltelli and Annoni, 2010; Pogson et al., 2012; Wang et al., 2013) of how single input parameters affect crop growth and yield formation. For supporting drought management, if the weather data can be input into crop models, the drought-induced changes of soil moisture and yield losses can be estimated. Most of the existing methods of providing future weather data as model inputs are based on historical data. For example, Du Toit and Du Toit (2003) compared the current weather conditions with historical data to identify the five best fitting years, and used the daily data for the rest of growing season from these five analogue years. Bannayan et al. (2003) applied a weather generator to create future weather data based on the stochastic analysis of multiple-year historical data, and later they (Bannayan and Hoogenboom, 2008) developed a weather analogue tool for predicting daily weather data based on a modification of the k-nearest neighbor approach. In the current research, in addition to historical weather data, we applied a scenario analysis approach to address the uncertainties of drought development (Refsgaard et al., 2007; Warmink et al., 2010) and to provide information about the potential consequences for decision makers if a given drought scenario is realized.

Beyond the efforts in yield forecasting, there is a need to facilitate analysis of past drought probability and permit dynamic analysis of future drought scenarios. First, a stochastic analysis of the drought probability is fundamental in risk management because risk generally is considered as a combination of probability and damage (Haynes et al., 2008). Second, using return periods (e.g., a 100-year drought) for evaluating the severity of a natural hazard is a widely accepted measurement for the public and decision makers. Quantitative analyses of drought return periods date to work of Yevjevich (1967), who proposed the run concept for identifying drought events and their statistical characteristics. Most of these research efforts have been to derive drought return periods based on hydrological series (Sen, 1980; Sharma, 1997; Clausen and Pearson, 1995; Shiau and Shen, 2001; Shiau et al., 2007; Tarawneh and Salas, 2009) or meteorological data (Gabriel and Neumann, 1962; Serinaldi et al., 2009; Mirakbari et al., 2010; Núñez et al., 2011). For decision support of agricultural drought, however, it is necessary to evaluate return periods based on drought-induced yield losses. In addition, return periods are geographically scale-dependent. For example, if a 100-year drought occurs in a state, it does not imply the same severity for each county within this state; instead, the county-level drought may be more or less severe than the 100-year event. Quantitative evaluations of such scale-dependent return periods have rarely been reported.

The objectives of the current paper are to describe a Drought Risk Analysis System (DRAS) that allows the dynamic evaluation of large-scale yield losses and the calculation of scale-dependent return periods for agricultural droughts based on yield prediction. Using scenario analysis approaches, we applied the proposed system to quantify drought impacts on corn yields during the 2012 drought in the U.S.A. and to the 2000 and 2009 droughts in Liaoning Province, China. Remote sensing data were also used for dynamic verification of the modeled results.

Section 2 introduces the methodology of the dynamic evaluation and prediction of drought-induced yield losses, as well as the software tool for supporting dynamic agricultural drought management. Section 3 demonstrates applications of the tool for evaluating the daily impacts of the 2012 drought on corn in the U.S.A., which applications are associated with remotely sensed information. Section 4 illustrates the case of the droughts in Liaoning Province, China, with a focus on the dynamic quantification of spatially scale-dependent drought return periods based on yield losses. The dynamic evaluation of the uncertainty of

drought impacts on crop growth is also demonstrated in the case study.

2. Model, methodology, and software

2.1. The DNDC model

The model adopted in the current research is DNDC (DeNitrification-DeComposition), which was developed at the University of New Hampshire. This model was initially developed for quantifying greenhouse gas emission from agricultural ecosystems (Li et al., 1992), and it was widely applied for yield prediction in later researches (e.g., Babu et al., 2005; Tonitto et al., 2007; Fumoto et al., 2008). Crop growth in the DNDC model is tracked by simulating the process of crop nitrogen (N) uptake from the environment, considering stresses from water and temperature. The sources and dynamic biogeochemical processes of soil N modeled in DNDC include biological nitrogen fixation, nitrification, de-nitrification, decomposition of organic matter, atmospheric nitrogen deposition, atmospheric NH_3 concentration, and fertilization from human inputs.

An optimal biomass accumulation curve (see details in Li et al., 1994; Kröbel et al., 2011) is used to calculate the maximum rate of daily biomass increase as well as the potential nitrogen and water demands according to user-defined parameters. Such parameters include the maximum yields, the crop water requirements (CWR), the optimal temperature for growth, the required cumulative temperature (or TDD: the thermal degree days), the biomass partitions and their C/N (carbon/nitrogen) ratios. The metric of thermal degree days (TDD) is used to define the growing duration and the plant growth index (PGI) by taking the input weather data into account. The PGI is a ratio (0–1) of the up-to-date accumulative temperature ($\sum$dT) to TDD, namely PGI = $\sum$dT/TDD. The crop matures when the PGI reaches 1.

In addition to the availability of N from multiple sources, the daily biomass growth is also related to the availability of water. The model simulates changes in soil moisture, the water movement in multiple soil layers according to the soil properties, and evapotranspiration using the Penman–Monteith equation. If the N or H_2O that is taken up cannot meet the respective daily potential demands, the crop biomass accumulation will be constrained from the optimal curve. Temperature stress is defined through the user-specified optimal temperature and the range of tolerance. The grain starts to grow if PGI >0.5. According to the user-defined maximum grain yield, the daily increase in grain biomass is determined by the potential grain increase and the stresses from nitrogen, water and temperature. The model allows the crop to recover if the nitrogen and/or water stresses are relaxed. The technical details of the model are found in multiple publications (e.g., Li et al., 1994; Zhang et al., 2002; Kröbel et al., 2011) and the DNDC User Guide (www.dndc.sr.unh.edu).

In any crop-growth model for large-scale yield prediction, in addition to accuracy, the availability of model inputs is a key issue. The performance of DNDC in yield prediction has been validated at both field and regional scales worldwide (e.g., Zhang et al., 2002; Babu et al., 2005; Tonitto et al., 2007; Fumoto et al., 2008; Kröbel et al., 2011). We adopted this model because it has a great strength in simulating the soil nitrogen and water processes, and because large-scale agricultural databases for the model have been established. Such agricultural databases (see the DNDC User Guide, www.dndc.sr.unh.edu) typically include daily weather data, soil properties (bulk density, pH, SOC, clay ratios), crop parameters (e.g., the maximum grain, biomass, C/N ratios, water demands, TDD, and planting-harvest dates), and management (e.g., fertilization and irrigation). For evaluating model performance, we use a part of historical climate and yield data to calibrate the model parameters such as water requirements, maximum yield, TDD, and harvest index, and then use another part of the data for model validation.

2.2. Methodology

This subsection introduces the methods for handling uncertainties in drought development based on scenario analysis and the approaches for deriving scale-dependent return periods.

2.2.1. Scenario-based assessment of dynamic yield losses

When using crop models to predict drought impacts on yield, a major source of uncertainty is the unknown duration of drought development. When a drought event occurs, information from short-term weather forecasts is usually insufficient to predict how long the drought will last. We used contingency analysis to address this uncertainty. As shown in Fig. 1, the climate conditions (e.g., precipitation and temperature) for the entire growing season of crops can be divided into known and unknown zones according to the current time. Monitoring networks can provide dynamic data for the model to quantify environmental impacts on crop yields retrospectively. With the passage of time, the known zone becomes larger, and the unknown zone becomes smaller. For future drought impacts in the unknown zone, as discussed previously, a possible approach is to generate weather data as inputs to simulate possible consequences. In the current research, we set up multiple scenarios (e.g., S0, S10, S20, … Sn) for the DNDC model to calculate potential changes in crop yield. The unknown future (Fig. 1) can be divided into multiple contingency levels to forecast crop yields and support appropriate decision making.

In this study, different drought scenarios were specified in the DNDC model: (1) the drought stops instantly without further water stress for the rest of the growing season (i.e., S0 in Figs. 1 and 2); (2) drought continues in a given period of time (e.g., in the next 10, 20, 30, or 50 days), with no more water stress thereafter; and (3) drought changes with the weather conditions found in the historical daily data that represent typical dry, medium or wet years. After receiving the daily data, the model updates the input variables and then conducts scenario analysis. The S0 scenario allows the

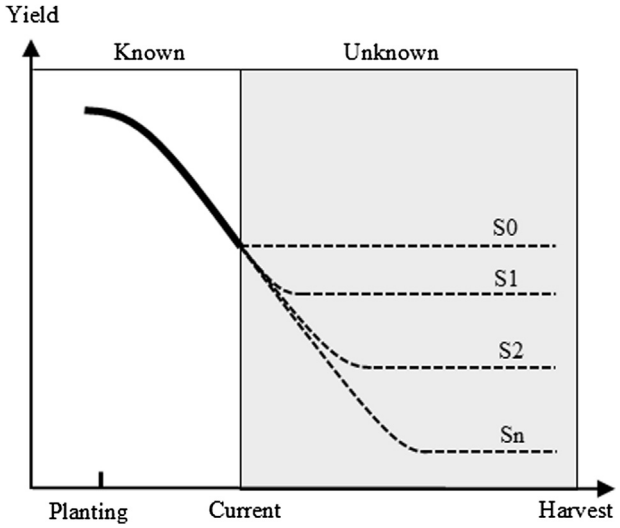

Fig. 1. The conceptual design for analyzing the uncertainty of drought impacts on crop yields. With dynamic monitoring data input, the environmental conditions before the current time are known, but unknown thereafter. For the future, we assume several scenarios (S0, S10 … Sn). Combining the past known input variables and the future data, potential yield changes under different scenarios can be estimated.

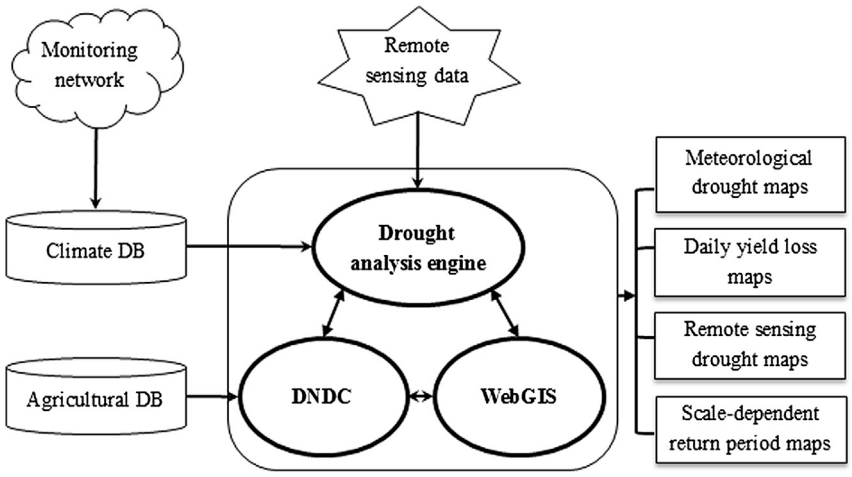

Fig. 2. The main structure of the Drought Risk Analysis System (DB: database).

estimation of the yield losses a drought has caused up to the current date. This is because in the S0 scenario, the model simulates the crop growth with the monitoring data in the known zone, and continues to simulate the growth and grain formation until harvest without any water stress. In this scenario, the model always calculates the daily maximum water requirements, generates the needed amount of water as an input for daily crop growth, and then uses the daily temperature data averaged from historical records for the rest of the growing season. Therefore, the derived yield loss in the S0 scenario (in Fig. 1) is considered to be the up-to-date yield loss, and this loss cannot be recovered even if the water supply is sufficient in future.

Given the yield losses in S0, it is also possible to calculate the extra yield losses in a scenario if the drought continues. For example, in a 10-day drought scenario (e.g., S10 in Fig. 1), the model considers the precipitation to be zero and the daily temperatures to be the historically high values in the next 10 days. The model uses such climate data to simulate crop growth for these 10 days, and then supplies sufficient water afterward for ideal growth until harvest. The calculated yield change (S10) from S0 is considered to be the loss induced by the following 10-day drought.

There are different methods for determining the typical dry, medium, or wet years for scenario analyses. In Liaoning Province of China, for example, the department of water resources defines these years for each county by using historical climate data in hydrological analysis. However, in this paper these definitions were not adopted because a typical hydrological year does not necessarily correspond to a typical agricultural year. Instead, we used 50-year daily climate data to run the model for generating a yield series dataset after finishing the validation of the DNDC model. From this dataset, a year with the yield value close to the average yield is considered a medium year; and a year with lowest or highest yield can be considered a typical dry or wet year. These typical years are manually confirmed with the actual precipitation records, and they are recorded in the county-level agricultural database so that the model can retrieve the daily data from the defined typical years as inputs for scenario analysis.

2.2.2. Quantifying scale-dependent return periods

Drought signals derived from meteorological and hydrological information may underestimate the severity of drought effects during the water-sensitive stages for grain formation, or may overestimate impacts in other stages. Because our method allows for the dynamic evaluation of drought-induced yield losses, we quantified agricultural drought return periods based on yield prediction during a drought event for the case study of the Liaoning Province using the following steps.

Firstly, after calibration and validation of the model, we used the daily climate data (precipitation and temperature) from 1960 to 2009 in the model to generate a 50-year corn yield series for each county based on a baseline of the current crop parameters, soil status and management data. The prefecture-level and province-level yield series data were summarized from the county-level results. Therefore, every geographic region at different scales has its own yield series data.

Secondly, based on the yield series datasets, we determined that the GEV (generalized extreme value) distribution can generate the best-fitting curves for the counties, the prefectures, and the province. This distribution was selected from over 50 different types of probability distributions according to the Anderson–Darling test by using the software EasyFit (www.mathwave.com). The probability density function $f(x)$ for a GEV distribution can be expressed with equation (1), and its cumulative distribution function $F(x)$ is defined in equation (2). For the drought situation, if the yield loss is x, the return period $T = 1/F(x)$.

$$f(x) = \begin{cases} \frac{1}{\sigma}\exp\left(-(1+kz)^{-1/k}\right)(1+kz)^{-1-1/k} & k \neq 0 \\ \frac{1}{\sigma}\exp\left(-z-\exp(-z)\right) & k = 0 \end{cases} \quad (1)$$

$$F(x) = \begin{cases} \exp(-(1+kz)^{-1/k} & k \neq 0 \\ \exp(-\exp(-z)) & k = 0 \end{cases} \quad (2)$$

where μ is the location parameter of the maximum $f(x)$; k is the shape parameter, σ as the scale parameter, and $z = (x\text{-}\mu)/\sigma$.

Finally, using the derived 50-year corn yield datasets, we applied the EasyFit tool to generate the GEV parameters of μ, σ and k for the best-fitting curve for each administrative division. Once the values of μ, σ and k are defined for a geographic region, the return-period values for this region can be calculated according to the modeling results of drought-induced yield losses.

2.3. Software: The Drought Risk Analysis System

Based on the DNDC model and the scenario-based dynamic drought analysis approach, a software system entitled Drought Risk Analysis System (DRAS) was developed to allow dynamic analysis of drought-induced yield losses. This system can also map remote-

sensing-based drought areas, meteorological drought areas, and yield-based drought return periods.

Fig. 2 shows the data flow and the main structure of the agricultural Drought Risk Analysis System (DRAS). It includes three modules: the DNDC model, a drought analysis engine, and a web-based geospatial tool (WebGIS). The input data can be read from climate databases, agricultural databases, and remote sensing data. The climate database can be further connected with the monitoring network. The drought analysis engine plays a pivotal role in managing the data flow, running the model, and publishing the resulting maps on the web. This system was first installed in a drought management office in Liaoning Province, China in 2012. When the monitoring data are received by the climate database every day, the drought analysis engine automatically reads the new data, checks for data errors, and converts the data into the DNDC input-data formats. It then uses the DNDC model to simulate crop growth according to the predefined scenarios. Once the modeling tasks are completed, the drought analysis engine transfers the modeling results into map formats and delivers the maps to WebGIS for online publication. Currently remote sensing data are still based on manual access to the data sources and relatively independent data processing. Many functions (e.g., data conversion and data mapping) in the current version of this system were still specifically designed for the Liaoning Province. A more generic version is under development that will allow dynamic publication of modeling results via the Internet.

3. Case 1: dynamic yield prediction in the 2012 U.S.A. drought

In 2012, the worst drought since the 1950s had affected 84% of the corn growth in the United States (USDA, 2012a). In July, the USDA declared more than 1000 counties to be drought disaster areas, and global corn prices surged nearly 23% (USDA, 2012b). While the USDA released monthly predictions of grain yields to the public, it was difficult to know how the drought would further affect the grain yield. Based on a well-established database of county-level soil, fertilization, and crop parameters, we started collecting the additional data required by DNDC, calibrating and verifying the model in June, 2012. In September and October, we applied the model to predict corn yields. The predicted results (Figs. 3–5) were presented in a meeting conducted in the office of the U.S.A. National Agricultural Statistics Service (NASS) on November 19th, 2012.

The agricultural crop database for the United States has been designed for model inputs. The soil data were from the U.S.A. Natural Resources Conservation Service (NRCS, http://sdmdataaccess.nrcs.usda.gov/, accessed on July 07th, 2014). The historical county-level data of management, corn yields, and harvested areas were from the USDA (www.nass.usda.gov/Data_and_Statistics/index.asp, accessed on July 07th, 2014), and the climate data from NOAA (www.ngdc.noaa.gov/ngdcinfo/onlineaccess.html, accessed on July 07th, 2014). A part of the climate and yield data between 2000 and 2011 were used for model calibration, and another part for model verification. Remote sensing data were used to separate irrigated and rainfed corn fields and to downscale the county-level model estimation to 500 m resolution via spatial interpolation. The products applied in the current research include the 30 m corn maps in USDA Cropland Data Layer datasets produced from multi-sensor imagery (Han et al., 2012), and the 250 m irrigation maps in USGS derived from MODIS data (Pervez and Brown, 2010). In addition, MODIS 8-day 1 km LAI data from USGS (Myneni et al., 2002) after time-series fitting (Jonsson and Eklundh, 2004) were compared with model estimates.

Fig. 3 shows the modeled corn yields for the entire U.S.A. using the 2012 daily weather data from June to October. After receiving daily data, a best-case scenario (S0) was applied. Additionally, we used the model with daily-generated scenario data to assess potential, future drought-induced losses. For example, on July 1st (Fig. 3), the modeled national corn yield was 157 bushel/acre if the drought ceased. It declined further to 149, 139, or 130 bushel/acre under scenarios of continued drought for 10, 20, or 30 days (i.e., the S10, S20, or S30 scenarios), respectively. In Fig. 3, the black line represents the modeled daily corn-yield changes (S0) in the United States, which in general, agrees with the monthly projected yields (i.e., the red line) by NASS. By the end of October, 2012, the model predicted an average corn yield of 120 bushels/acre, which was remarkably close to the 123 bushels/acre as reported by the USDA in February 2013.

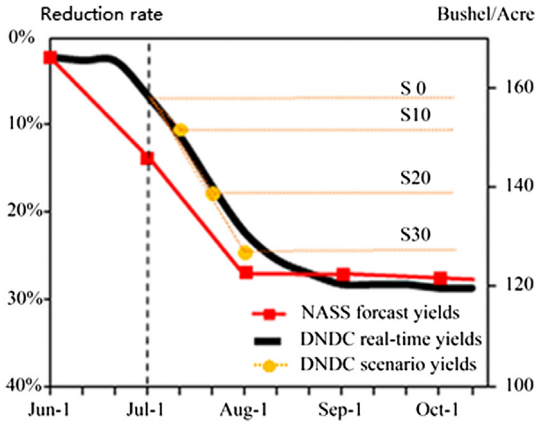

Fig. 3. The black line represents the modeled daily corn yield losses (S0) in the United States during the 2012 drought, and the red line is the monthly yield forecast by NASS. The orange lines are an example of scenario analysis by assuming that the current time is July 1st, and the expected maximum corn yield would be S0 if the drought stops immediately, and S10, S20, or S30 if the drought continues in the next 10, 20, or 30 days. (For interpretation of the references to colour in this figure legend, the reader is referred to the web version of this article.)

Fig. 4 illustrates the spatial distributions of the daily corn-yield losses in the Corn Belt, and the daily projected yield losses under the scenarios without rainfall during subsequent 10 and 30 days. The results show that the scenario map with an extra 30-day drought on June 1st is consistent with geographical patterns as of July 1st yield-loss, after update from the observation data; and the 30-day scenario map of July 1st is consistent with August 1st yield loss. This indicates that the drought in these periods of time was close to the worst case. After mid-August, the total yield losses (Fig. 3) and their distributions (Fig. 4) become highly certain, showing minimal changes up to harvest time.

The modeled results were compared with dynamic information from remote sensing to enhance our understanding of crop development in response to drought. Fig. 5 shows the anomalies of Leaf Area Index (LAI) retrieved from Moderate Resolution Imaging Spectrometer (MODIS, i.e., the 8-day data series from 2001 to 2012), which have similar geographic distributions to the modeled biomass anomalies from DNDC in both space and time during the drought. In Fig. 5, some differences between the modeled results and LAI are evident. The irrigated areas in the southeast of Nebraska (denoted by white circles) were assumed to be unaffected by the drought in our model, but experienced large LAI anomalies from MODIS in August. According to the NASS yield reports, the drought impact in this area was relatively small, demonstrating that the model generated a better prediction than that would have been inferred from MODIS LAI. The southeast corner of North Dakota (marked with the green circle) experienced a long-lasting but moderate drought, and the model predicted moderate impact on corn biomass and yield in this area. This impact was not apparent

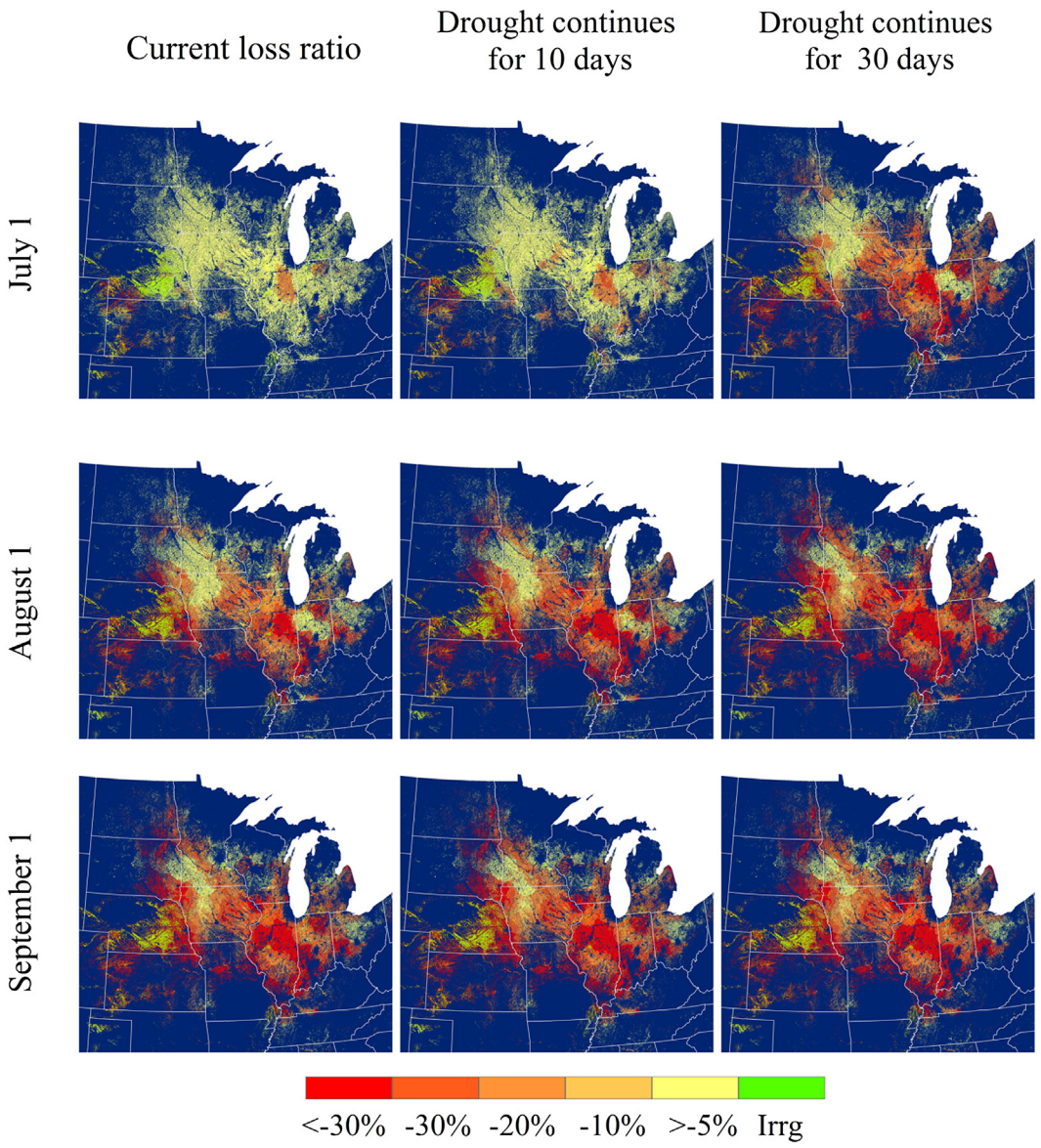

Fig. 4. Distributions of the expected daily corn yield losses (the modeled yield departure from the average county-level values of 2000–2011) in the Midwest Corn Belt for three reference dates; and the projected yield changes under the scenarios with continuous drought in the next 10 days and 30 days (map resolution: 500 m). The green areas represent the irrigated corn fields, without yield losses. (For interpretation of the references to colour in this figure legend, the reader is referred to the web version of this article.)

from MODIS LAI until August. The yield loss was overestimated in DNDC when compared with NASS reports. This suggests that the integration of remote sensing data and crop modeling can assist in the identification of modeling errors.

Following the release of the 2012 harvest data by the USDA, we found that the model was able to make accurate prediction of corn yields over large areas. At the national level, the modeled reduction in U.S.A. corn production was 18% of the average yield in 2000–2011. Yield was predicted at 120 bushel/acre, with 98% similarity of that reported by the NASS (123 bushel/acre) in February 2013. At the state level, the modeled values of corn yield corresponded well with actual harvest values (Fig. 6). The modeling indicated that irrigation played an important role in moderating the drought impacts on many corn-producing regions located in the South, West and Midwest states. Overall, irrigation offset 7% of the nationwide drought damage.

The model can also be used to explain the detailed drought impacts on crop-development processes in any specific county. Fig. 7 demonstrates the daily biomass growth and crop water stress in 2012 for two typical corn-producing counties: Nobels County in Minnesota (Fig. 7-A) and Woodford County in Illinois (Fig. 7-B). These modeling results show that severe water stress started at the end of June in Woodford and in early July in Nobels. Similar patterns of drought impacts were captured at the regional scale for the corn-producing states. The prolonged water stress substantially reduced yields in July and August when the crop was in tasseling and silking stages, which are especially sensitive to water stress. From the daily outputs, users can understand how the processes of biomass and yield formation in 2012 differ from other years. The differences are illustrated for 2007 in Fig. 7.

4. Case 2: scale-dependent dynamic drought return periods in Liaoning, China

Liaoning Province is located in the northeast of China (Fig. 8a), with a total terrestrial area of 148 thousand km^2. This province

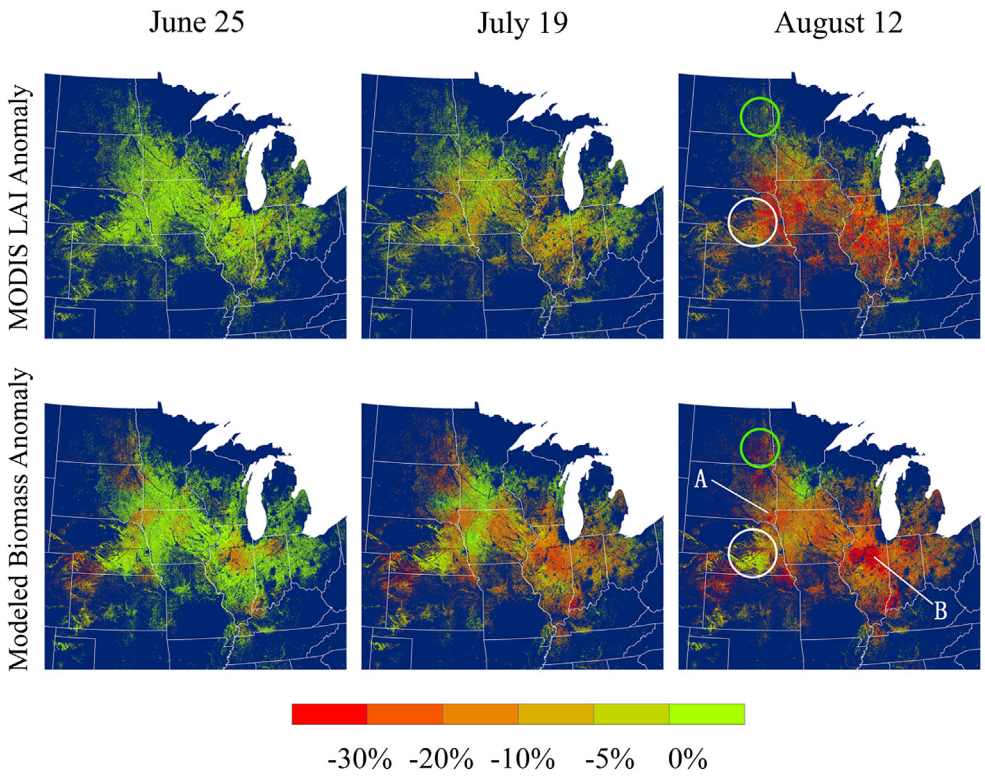

Fig. 5. The MODIS LAI anomaly (departure from the average values of 2007–2011), and the DNDC modeled biomass anomaly in 2012 for the U.S.A. corn fields (map resolution: 500 m). The Green and white circles indicate two places with great differences between the MODIS and DNDC signals. A and B show the locations of the Nobels County of Minnesota and the Woodford County of Illinois for Fig. 7 (For interpretation of the references to colour in this figure legend, the reader is referred to the web version of this article.)

includes 15 prefectures, 19 county-level urban regions, and 81 counties with agriculture production. Its annual precipitation ranges from 450 to 1100 mm (Fig. 8b). Drought events occur frequently in the northwestern part of the province but are rare in the east. In recent years, the planted areas of corn, rice and soybean have represented approximately 70%, 18%, and 5% of the total farmland, respectively. Most corn and soybean are rainfed. We started developing the scenario-based analysis approach for dynamic evaluation and prediction of drought-induced yield losses in a case study on the northwestern Liaoning in 2009 and then extended it to the entire province. The first version of the Drought Risk Analysis System (DRAS) was installed in a drought management office in Liaoning Province, China, in 2012. We use the 2000 and 2009 droughts as a case study. Output results similar to those illustrated in the case study in the U.S.A. can be delivered to the relevant decision-making office. This section focuses on dynamic evaluation of the spatially scale-dependent return periods based and the daily predicted corn yield losses in the Liaoning Province.

As described in the methodology section, we used 50-year yield series data to generate the GEV parameters of μ, σ and k for the best fitting curve in each geographic region. Once these parameters were determined, a return period was calculated by using the modeling result of drought-induced yield loss. Fig. 9a, for instance, illustrates the calculated return periods of drought-caused corn yield losses for the entire Liaoning Province from 1960 to 2009. The result indicates that the drought severity and frequency in this region after the mid-1990s have increased considerably during these 50 years.

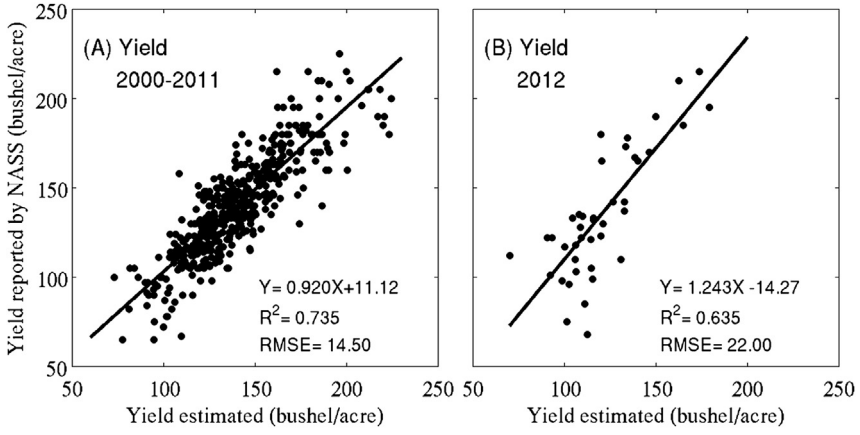

Fig. 6. Comparisons between the reported state-level corn yields from NASS and the estimated yields from modeling for (A) 2000–2011 and (B) 2012.

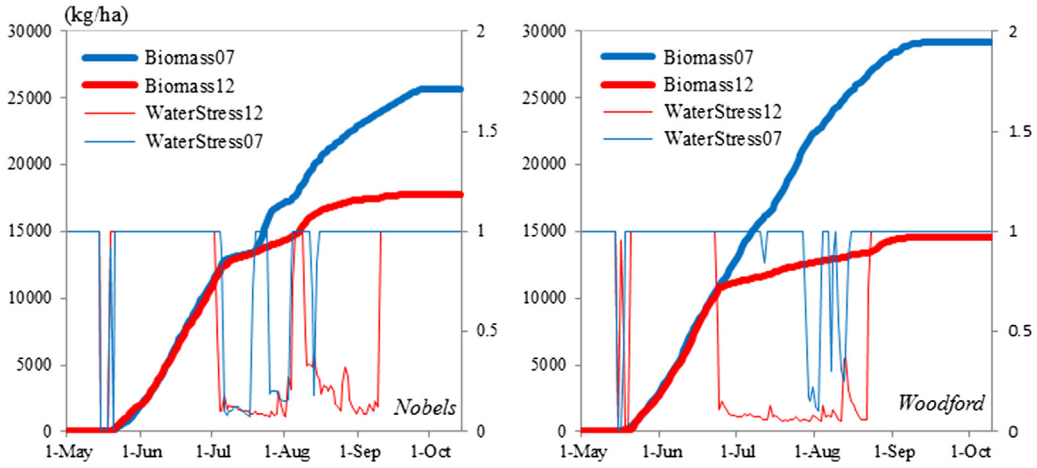

Fig. 7. Examples of the simulated processes of daily biomass (kg/ha) accumulation (Biomass12), and corn water stress (WatgerStress12) in the Nobels County of Minnesota (Fig. 5-A) and the Woodford County of Illinois (Fig. 5-B) in 2012, compared with a moderate year in 2007 (Biomass07 and WatgerStress12). Water stress means the ratio of the daily crop water taken from the soil to the potential transpiration (1: no stress, 0: extreme stress).

Using the 2000 and 2009 drought events as examples, we demonstrate that the return periods depend on the geographic scale. Fig. 9b shows that the modeled corn yields compared with the measured values recorded in the statistical yearbooks. Fig. 10 displays the modeled daily changes of the return periods in at the province, prefecture, and county levels based on the yield prediction in the S0 scenario in Fig. 1. The province encountered a widespread drought in 2000. The modeling results indicate that it was a 127-year drought for the province on the harvest time, although the return periods were less than 100 years for most counties and prefectures. Most of the yield losses in the 2000 drought occurred in July and August during the corn flowering and grain setting stages. In 2009, only a part of counties were affected by the drought. While the return periods in the two western prefectures are more than 20 years, for the province it was only a 7-year drought. Using the scenario-analysis approach (Fig. 1), the Drought Risk Analysis System can also predict the changes of return periods if the drought continues for a given period of time. Such dynamic and scale-dependent information can help institutions responsible for drought management in assessing the drought impacts within their administrative boundaries and responding rationally during the drought.

The Drought Risk Analysis System (DRAS) can also provide useful information for users to dynamically identify the uncertainty of drought impacts. Fig. 11 shows an example of the daily evaluation of the uncertainty during the 2009 drought in Chaoyang County, located in the west of Liaoning Province. Using the historical climate data from typical dry, moderate, or wet years (see Section 2.2) as the upcoming weather scenarios thorough harvest, it is possible to identify the range of biomass changes between the scenarios. As illustrated in Fig. 11, in the early stage (June 15th), the range between the wet-year and dry-year scenario are large, but the range decreases with time. On August 15th, the yield loss becomes highly certain no matter how much rainfall is received thereafter. As long as the model performance is reliable, it can provide users with valuable information to evaluate the uncertainty of drought impacts on crop growth.

5. Discussion

This study developed a scenario-based approach to the dynamic evaluation of the uncertainties associated with predicting drought-induced yield losses, a method for scale-dependent assessment of drought return periods based on yield information, and a software tool (the Drought Risk Analysis System) based on the DNDC model. The daily maps of the modeling results can help users understand the changes and distributions of the current yield losses and the potential consequences of different scenarios for drought

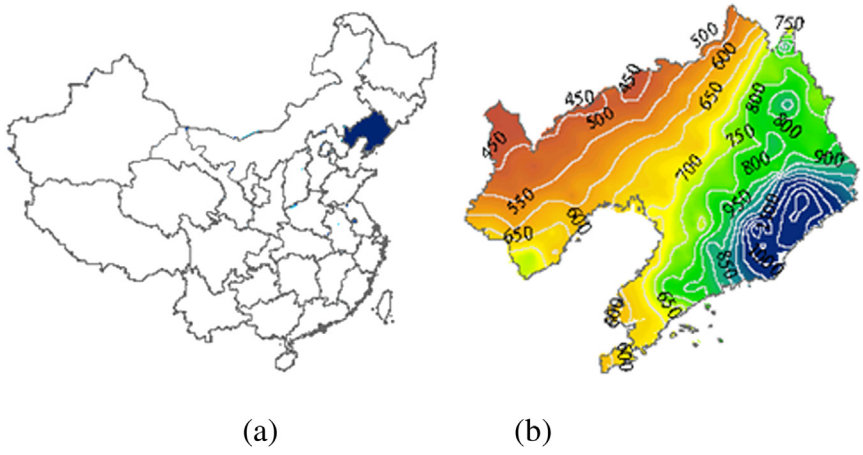

Fig. 8. (a) The mainland of China, and the location of Liaoning Province; (b) the average annual precipitation in Liaoning (mm).

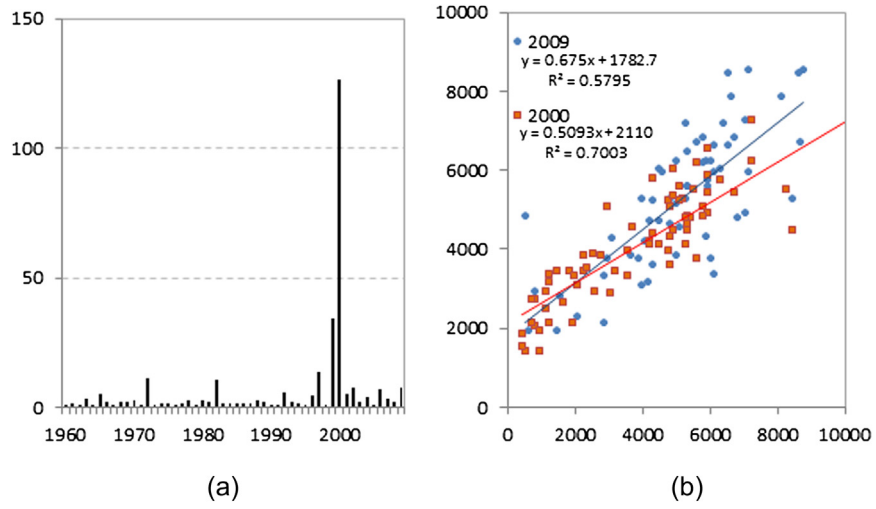

Fig. 9. (a) The calculated return periods of drought-induced corn yield losses for Liaoning Province; (b) the modeled (x) vs. the measured (y) county-level corn yields during the 2000 and 2009 drought events (units: kiloton).

development. Remote sensing can provide a direct measure of the drought-affected areas to allow users to confirm the modeling results during the drought. In addition to the broad-scale information, the system can also provide detailed information on the water-stress process and the uncertainty of biomass development at any specific site. The maps of the scale-dependent drought return periods are based on yield evaluation, and they can help decision makers at various levels evaluate the dynamics of drought impacts on agriculture. In comparison with the current approaches to evaluate the severity of droughts, the Drought Risk Analysis System (DRAS) can provide much more comprehensive, predictive, and detailed information on the consequences of drought impacts on food production.

Although the DNDC crop model performs reasonably for evaluating the drought impacts on yields, it does not consider factors such as disease, insect outbreaks, inundation, hail and hurricanes. These can create uncertainties when historical data are used for model calibration and validation. In irrigated farmlands, how farmers manage water resources remains unknown. In this paper, it was assumed that water was always sufficient for the irrigated lands, but this assumption could generate errors if the actual water resources were limited during the drought. Therefore, it is necessary to consider the timing irrigation and the amount of water applied as dynamic inputs to improve yield prediction.

In the future, several improvements could be made to the current study. First, based on the daily impact assessment, it is possible

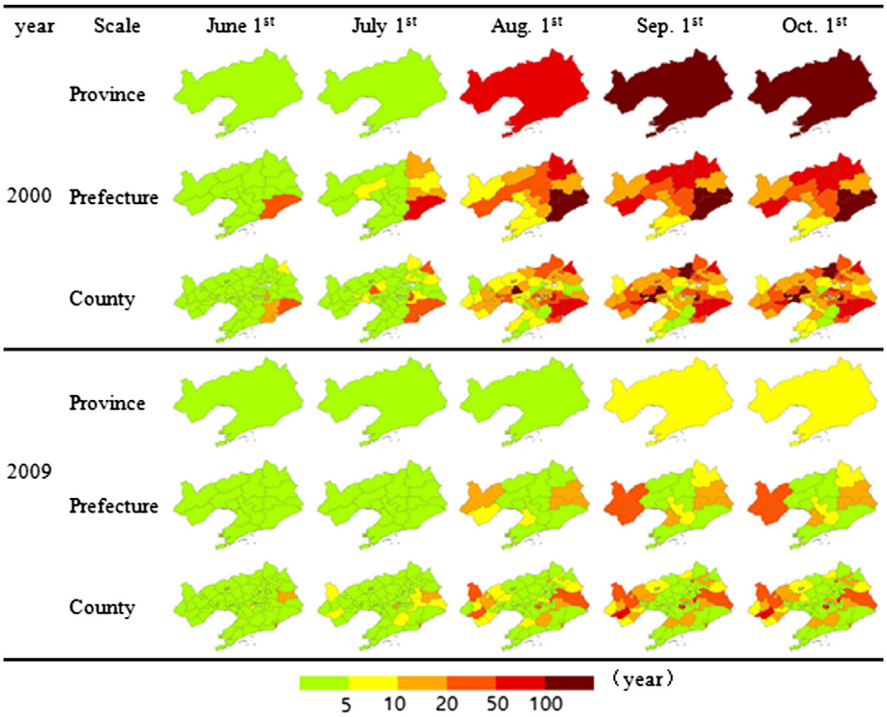

Fig. 10. The daily evaluation of the scale-dependent drought return periods according to the dynamic prediction of drought-induced yield losses in the 2000 and 2009 drought events.

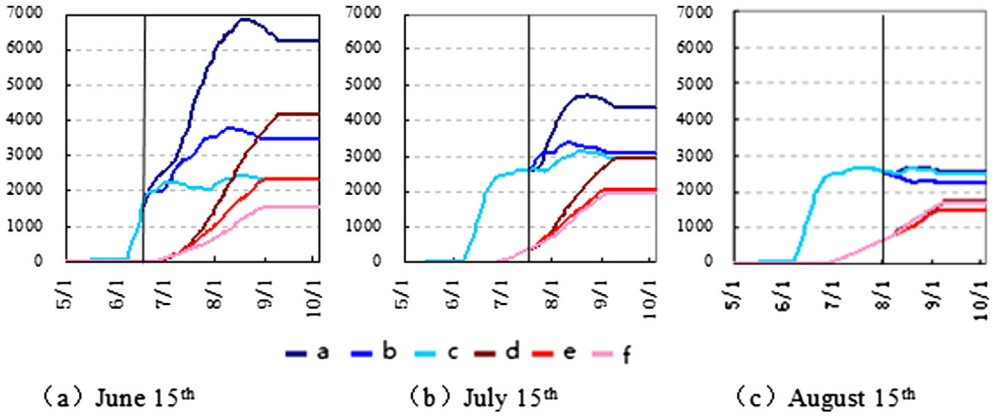

Fig. 11. Daily prediction of the biomass (kg/ha)development in Chaoyang County during the 2009 drought event using the historical data of the typical dry, moderate, or wet years. (a) the development of straw biomass using the typical wet-year data after the current day; (b) the development of straw biomass using the typical moderate-year data; (c) the development of straw biomass using the typical dry-year data; (d) the development of grain biomass using the typical wet-year data; (e) the development of grain biomass using the typical moderate-year data; (f) the development of grain biomass using the typical dry-year data.

to couple the crop modeling results with the medium-term climate prediction from climate modeling and thus evaluate the probabilities and risks of different drought scenarios for better decision support. Second, we have begun to extend the data beyond the geographic regions of Liaoning and the U.S.A., and we started to extend the model and associated databases to all of China and to include corn, wheat, and rice. It would be possible to build a global agricultural drought assessment system for the dynamic prediction of the worldwide grain production. Finally, irrigation is crucial in many counties, so adding a more sensitive treatment of irrigation by building broad-scale hydrological models in the Drought Risk Analysis System would improve its ability to evaluate dynamic changes to the water resources and enhance agricultural water management.

Acknowledgments

We gratefully acknowledge the support of the China 973 project 2013CB956600, CNSF#41371491, Tsinghua 20121088052, 2013M540087 and SEPA201309062. We appreciate all the help provided by China IWHR and the Office of Liaoning FCDRH. Thanks also go to the anonymous reviewers for their insightful comments.

References

Babu, Y.J., Li, C., Frolking, S., Nayak, D., Datta, A., Adhya, T., 2005. Modelling of methane emissions from rice-based production systems in India with the denitrification and decomposition model: field validation and sensitivity analysis. Curr. Sci.-Bangalore 89 (11), 1904.

Bannayan, M., Crout, N., Hoogenboom, G., 2003. Application of the CERES-Wheat model for within-season prediction of winter wheat yield in the United Kingdom. Agron. J. 95 (1), 114–125.

Bannayan, M., Hoogenboom, G., 2008. Weather analogue: a tool for real-time prediction of daily weather data realizations based on a modified k-nearest neighbor approach. Environ. Model. Softw. 23, 703–713.

Becker-Reshef, I., Vermote, E., Lindeman, M., Justice, C., 2010. A generalized regression-based model for forecasting winter wheat yields in Kansas and Ukraine using MODIS data. Remote Sens. Environ. 114 (6), 1312–1323.

Bolton, D.K., Friedl, M.A., 2013. Forecasting crop yield using remotely sensed vegetation indices and crop phenology metrics. Agric. For. Meteorol. 173, 74–84.

Boogaard, H., Van Diepen, C., Rötter, R., Cabrera, J., Van Laar, H., 1998. WOFOST 7.1: User's Guide for the WOFOST 7.1 Crop Growth Simulation Model and WOFOST Control Center 1.5. DLO Winand Staring Centre, Wageningen.

Clausen, B., Pearson, C., 1995. Regional frequency analysis of annual maximum streamflow drought. J. Hydrol. 173 (1), 111–130.

de Wit, C.T., 1965. Photosynthesis of Leaf Canopies. Agricultural Research Report 663, 1965. PUDOC, Wageningen, The Netherlands, pp. 1–57.

du Toit, A.S., du Toit, D.L., 2003. Short description of the model statistical package and weather analogue program. In: White, J.W. (Ed.), Modeling Temperature Response in Wheat and Maize: Proceedings of a Workshop, CIMMYT, El Batán, Mexico, 23-25 April 2001, pp. 42–46.

Eitzinger, J., Trnka, M., Hösch, J., Žalud, Z., Dubrovsky, M., 2004. Comparison of CERES, WOFOST and SWAP models in simulating soil water content during growing season under different soil conditions. Ecol. Model. 171 (3), 223–246.

Fumoto, T., Kobayashi, K., Li, C., Yagi, K., Hasegawa, T., 2008. Revising a process-based biogeochemistry model (DNDC) to simulate methane emission from rice paddy fields under various residue management and fertilizer regimes. Glob. Change Biol. 14 (2), 382–402.

Gabriel, K., Neumann, J., 1962. A Markov chain model for daily rainfall occurrence at Tel Aviv. Q. J. Royal Meteorol. Soc. 88 (375), 90–95.

Gao, B.-C., 1996. NDWI—a normalized difference water index for remote sensing of vegetation liquid water from space. Remote Sens. Environ. 58 (3), 257–266.

Gilmanov, T.G., Parton, W.J., Ojima, D.S., 1997. Testing the 'CENTURY'ecosystem level model on data sets from eight grassland sites in the former USSR representing a wide climatic/soil gradient. Ecol. Model. 96 (1), 191–210.

Han, W., Yang, Z., Di, L., Mueller, R., 2012. CropScape: a Web service based application for exploring and disseminating US conterminous geospatial cropland data products for decision support. Comput. Electron. Agric. 84, 111–123.

Haynes, H., Haynes, R., Pender, G., 2008. Integrating socio-economic analysis into decision-support methodology for flood risk management at the development scale (Scotland). Water Environ. J. 22 (2), 117–124.

Heim, R.R., 2002. A review of twentieth-century drought indices used in the United States. Bull. Am. Meteorol. Soc. 83 (8).

Hunt, E.D., Hubbard, K.G., Wilhite, D.A., Arkebauer, T.J., Dutcher, A.L., 2009. The development and evaluation of a soil moisture index. Int. J. Climatol. 29 (5), 747–759.

Idso, S., Jackson, R., Pinter Jr., P., Reginato, R., Hatfield, J., 1981. Normalizing the stress-degree-day parameter for environmental variability. Agric. Meteorol. 24, 45–55.

Jonsson, P., Eklundh, L., 2004. TIMESAT—A program for analyzing time-series of satellite sensor data. Comput. Geosciences 30 (8), 833–845.

Jones, C.A., Kiniry, J.R., 1986. CERES-Maize: a Simulation Model of Maize Growth and Development. A & M University, College Station, 194 pp.

Kincer, J.B., 1919. The seasonal distribution of precipitation and its frequency and intensity in the United States. Mon. Weather Rev. 47 (9), 624–631.

Kiniry, J.R., Sanderson, M.A., Williams, J.R., Tischler, C.R., Hussey, M.A., Ocumpaugh, W.R., Read, J.C., Van Esbroeck, G., Reed, R.L., 1996. Simulating Alamo switchgrass with the ALMANAC model. Agron. J. 88 (4), 602–606.

Kogan, F., Yang, B., Wei, G., Zhiyuan, P., Xianfeng, J., 2005. Modelling corn production in China using AVHRR-based vegetation health indices. Int. J. Remote Sens. 26 (11), 2325–2336.

Kogan, F.N., 1995. Droughts of the late 1980s in the United States as derived from NOAA polar-orbiting satellite data. Bull. Am. Meteorol. Soc. 76 (5), 655–668.

Kröbel, R., Smith, W., Grant, B., Desjardins, R., Campbell, C., Tremblay, N., Li, C., Zentner, R., McConkey, B., 2011. Development and evaluation of a new Canadian spring wheat sub-model for DNDC. Can. J. Soil. Sci. 91 (4), 503–520.

Li, C., Frolking, S., Frolking, T.A., 1992. A model of nitrous oxide evolution from soil driven by rainfall events: 1. Model structure and sensitivity. J. Geophys. Res. Atmospheres (1984–2012 97 (D9), 9759–9776.

Li, C., Frolking, S., Harriss, R., 1994. Modeling carbon biogeochemistry in agricultural soils. Glob. Biogeochem. cycles 8 (3), 237–254.

Li, C., Salas, W., DeAngelo, B., Rose, S., 2006. Assessing alternatives for mitigating net greenhouse gas emissions and increasing yields from rice production in China over the next twenty years. J. Environ. Qual. 35 (4), 1554–1565.

Marcovitch, S., 1930. The measure of droughtiness. Mon. Weather Rev. 58 (3), 113.

McCown, R., Hammer, G., Hargreaves, J., Holzworth, D., Freebairn, D., 1996. APSIM: a novel software system for model development, model testing and simulation in agricultural systems research. Agric. Syst. 50 (3), 255–271.
McGuire, J.K., Palmer, W.C., 1957. The 1957 drought in the eastern United States. Mon. Weather Rev. 85 (9), 305–314.
McKee, T.B., Doesken, N.J., Kleist, J., 1993. The Relationship of Drought Frequency and Duration to Time Scales, Proceedings of the 8th Conference on Applied Climatology. American Meteorological Society, Boston, MA, pp. 179–183.
Mirakbari, M., Ganji, A., Fallah, S., 2010. Regional bivariate frequency analysis of meteorological droughts. J. Hydrolo. Eng. 15 (12), 985–1000.
Moulin, S., Bondeau, A., Delecolle, R., 1998. Combining agricultural crop models and satellite observations: from field to regional scales. Int. J. Remote Sens. 19 (6), 1021–1036.
Munger, T.T., 1916. Graphic method of representing and comparing drought intensities. Mon. Weather Rev. 44 (11), 642–643.
Murthy, C., Thiruvengadachari, S., Raju, P., Jonna, S., 1996. Improved ground sampling and crop yield estimation using satellite data. Int. J. Remote Sens. 17 (5), 945–956.
Myneni, R., Hoffman, S., Knyazikhin, Y., Privette, J., Glassy, J., Tian, Y., Wang, Y., Song, X., Zhang, Y., Smith, G., 2002. Global products of vegetation leaf area and fraction absorbed PAR from year one of Modis data. Remote Sens. Environ. 83 (1), 214–231.
Narasimhan, B., Srinivasan, R., 2005. Development and evaluation of Soil Moisture Deficit Index (SMDI) and Evapotranspiration Deficit Index (ETDI) for agricultural drought monitoring. Agric. For. Meteorol. 133 (1), 69–88.
NASS, 2009a. Guide to NASS Surveys and Programs - Agricultural Yield. http://www.nass.usda.gov/Surveys/Guide_to_NASS_Surveys/Agricultural_Yield/index.asp (accessed on 18.04.13.).
NASS, 2009b. Remotely Sensed Data for Crop Condition and Crop Yield (accessed on 18.04.13.). http://www.nass.usda.gov/Surveys/Remotely_Sensed_Data_Crop_Yield.
Núñez, J.H., Verbist, K., Wallis, J.R., Schaefer, M.G., Morales, L., Cornelis, W., 2011. Regional frequency analysis for mapping drought events in north-central Chile. J. Hydrol. 405 (3), 352–366.
Palmer, W.C., 1965. Meteorological Drought. US Department of Commerce, Weather Bureau, Washington, DC, USA.
Palmer, W.C., 1968. Keeping Track of Crop Moisture Conditions, Nationwide: the New Crop Moisture Index.
Palosuo, T., Kersebaum, K.C., Angulo, C., Hlavinka, P., Moriondo, M., Olesen, J.E., Patil, R.H., Ruget, F., Rumbaur, C., Takáč, J., 2011. Simulation of winter wheat yield and its variability in different climates of Europe: a comparison of eight crop growth models. Eur. J. Agron. 35 (3), 103–114.
Pervez, M.S., Brown, J.F., 2010. Mapping irrigated lands at 250-m scale by merging Modis data and national agricultural statistics. Remote Sens. 2 (10), 2388–2412.
Pogson, M., Hastings, A., Smith, P., 2012. Sensitivity of crop model predictions to entire meteorological and soil input datasets highlights vulnerability to drought. Environ. Model. Softw. 29 (1), 37–43.
Refsgaard, J.C., van der Sluijs, J.P., Hojberg, A.L., Vanrolleghem, P.A., 2007. Uncertainty in the environmental modelling process–a framework and guidance. Environ. Model. Softw. 22 (11), 1543–1556.
Sakamoto, T., Gitelson, A.A., Arkebauer, T.J., 2013. MODIS-based corn grain yield estimation model incorporating crop phenology information. Remote Sens. Environ. 131, 215–231.
Saltelli, A., Annoni, P., 2010. How to avoid a perfunctory sensitivity analysis. Environ. Model. Softw. 25 (12), 1508–1517.
Sen, Z., 1980. Statistical analysis of hydrologic critical droughts. J. Hydraul. Div. 106 (1), 99–115.
Serinaldi, F., Bonaccorso, B., Cancelliere, A., Grimaldi, S., 2009. Probabilistic characterization of drought properties through copulas. Phys. Chem. Earth, Parts A/B/C 34 (10), 596–605.
Sharma, T., 1997. Estimation of drought severity on independent and dependent hydrologic series. Water Resour. Manag. 11 (1), 35–49.
Shiau, J.T., Feng, S., Nadarajah, S., 2007. Assessment of hydrological droughts for the Yellow River, China, using copulas. Hydrol. Process. 21 (16), 2157–2163.
Shiau, J.-T., Shen, H.W., 2001. Recurrence analysis of hydrologic droughts of differing severity. J. Water Resour. Plan. Manag. 127 (1), 30–40.
Steduto, P., Hsiao, T.C., Raes, D., Fereres, E., 2009. AquaCrop—The FAO crop model to simulate yield response to water: I. Concepts and underlying principles. Agron. J. 101 (3), 426–437.
Svoboda, M., 2000. An introduction to the drought monitor. Drought Netw. News 12, 15–20.
Tarawneh, Z.S., Salas, J.D., 2009. The occurrence probability and return period of extreme hydrological droughts. In: Proceedings of the 13th International Water Technology Conference, Egypt, March 2009.
Tonitto, C., David, M.B., Drinkwater, L.E., Li, C., 2007. Application of the DNDC model to tile-drained Illinois agroecosystems: model calibration, validation, and uncertainty analysis. Nutrient Cycl. agroecosys. 78 (1), 51–63.
USDA, 2012a. Agricultural Weather and Drought Update – 8/16/12. http://blogs.usda.gov/2012/08/16/agricultural-weather-and-drought-update-%E2%80%93-81612/.
USDA, 2012b. Agricultural Weather and Drought Update – 7/12/12. http://blogs.usda.gov/2012/07/12/agricultural-weather-and-drought-update-%E2%80%93-71212/.
Wang, J., Li, X., Lu, L., Fang, F., 2013. Parameter sensitivity analysis of crop growth models based on the extended Fourier Amplitude Sensitivity Test method. Environ. Model. Softw. 48, 171–182.
Warmink, J., Janssen, J., Booij, M.J., Krol, M.S., 2010. Identification and classification of uncertainties in the application of environmental models. Environ. Model. Softw. 25 (12), 1518–1527.
Wilhite, D.A., 2005. Drought and Water Crises: Science, Technology, and Management Issues. CRC Press, Boca Raton: FL.
Wilhite, D.A., Buchanan-Smith, M., 2005. Drought as hazard: understanding the natural and social context. Drought and Water Crises–science, Technology and Management Issues. Taylor & Francis. ISBN 0 847(2771)1.
Williams, J.R., Singh, V., 1995. The EPIC model. Comput. Models Watershed hydrol., 909–1000.
Woli, P., Jones, J.W., Ingram, K.T., Fraisse, C.W., 2012. Agricultural reference index for drought (ARID). Agron. J. 104 (2), 287–300.
Yevjevich, V., 1967. An Objective Approach to Definitions and Investigations of Continental Hydrologic Droughts. Colorado State University, Fort Collins, Colorado. Hydrology paper 23.
Zhang, Y., Li, C., Zhou, X., Moore III, B., 2002. A simulation model linking crop growth and soil biogeochemistry for sustainable agriculture. Ecol. Model. 151 (1), 75–108.